CORA Cork Open Research Archive
Cartlann Taighde Oscailte Chorcaí

Title	Automatic ASET sensitivity evaluation of a custom-designed 180nm CMOS technology operational amplifier
Authors	Fontana, Andrés;Pazos, Sebastian M.;Aguirre, Fernando L.;Palumbo, Felix
Publication date	2017-10-05
Original Citation	Fontana, A., Pazos, S. M., Aguirre, F. L. and Palumbo, F. (2017) 'Automatic ASET sensitivity evaluation of a custom-designed 180nm CMOS technology operational amplifier', 2017 Argentine Conference of Micro-Nanoelectronics, Technology and Applications (CAMTA), Buenos Aires, Argentina, 27-28 July 2017, pp. 21-25. https://doi.org/10.1109/CAMTA.2017.8058136
Type of publication	Conference item;proceedings-article
Link to publisher's version	10.1109/camta.2017.8058136
Rights	© 2017, IEEE. Personal use of this material is permitted. Permission from IEEE must be obtained for all other uses, in any current or future media, including reprinting/republishing this material for advertising or promotional purposes, creating new collective works, for resale or redistribution to servers or lists, or reuse of any copyrighted component of this work in other works.
Download date	2026-11-01 13:17:19
Item downloaded from	https://hdl.handle.net/10468/18021



UCC
University College Cork, Ireland
Coláiste na hOllscoile Corcaigh

Automatic ASET sensitivity evaluation of a custom-designed 180nm CMOS technology Operational Amplifier

Andrés Fontana, Sebastián M. Pazos, *Student Member, IEEE,* Fernando L. Aguirre, *Student Member, IEEE,* Félix Palumbo, *Member, IEEE,*

***Abstract*—This work presents a SPICE-based automatic SET sensitivity evaluation of a 180nm CMOS full-custom Operational Amplifier. The set-up uses the well known double exponential current law to inject SET into every sensitive node in the circuit hierarchy. The pulse parameters are obtained according to a previously generated population of particles with randomly assigned energies and species, the node bias condition at the instant of the strike and an empirical model obtained through TCAD simulations. The circuit is evaluated transistor-wise for each ion of the generated database and the output waveforms are processed in time and frequency domain to obtain figures of merit of the hardness of the proposed design on a given radioactive environment. Results allow to identify the most sensitive devices and the expected error rate for the projected application, allowing to conduct hardening techniques during early design stages.**

***Index Terms*—ASET, Analog CMOS, SPICE, Heavy Ions**

I. Introduction

RADIATION effects in Integrated Circuits (ICs) have been studied since the early years of integration technology. Initially, Total Ionizing Dose (TID) was the main concern due to its negative effects on device parameters, specially in the case of CMOS technologies. As the feature sizes scaled down, Complementary Metal-Oxide-Semiconductor (CMOS) devices started showing a higher resilience to TID effects and the concerns of the scientific community migrated to another, early predicted phenomenon: the Single Events (SE).

Produced by the impact of a neutron or a high energy charged particle, SE are the result of the interaction between these particles and the constructive materials of ICs. In a general manner, these particles loose a significant amount of energy by ionization, generating free carriers in the semiconductor, alongside with secondary emission of X-Rays, secondary ions, delta electrons, etc [1]. Although its existence was known on the early 60s [2], [3], SE did not represent a crucial reliability concern back then, simply because the sizes of the circuit devices were big enough to make the charge deposition negligible from the point of view of the device operation. Nevertheless, scaling contributed to make these effects more important as a reliability hazard in ICs. The transient behaviors resulting from charge deposition on semiconductors, namely Single Event Transients (SET), started to be considerable for the normal operation of circuits, but its influence is strongly dependent not only on the nature of the particle that impacts a device (energy and species), but with the design topology [4], constructive technology and technological parameters [5], speed of the circuit and biasing, layout topology, etc. This conglomerate of variables has driven many research groups to model SET on different abstraction levels in order to account for them on early design stages of ICs.

To the date, several tools for the simulation of SET on ICs can be found described in the literature [6]. Many of these tools make use of finite element method simulations implemented in Technology Computer Assisted Design (TCAD) software. Though very accepted in the academia, TCAD simulations are quite time and resource consuming, considering that precise simulation of SE Effects (SEE) require refined meshes and complex 3D structures for the solvers to yield exact and valid results. It should be added that the main focus of these tools are Single Event Upsets (SEU) in memory devices, which are physically regular structures where the metric of interest is perfectly identified to be the Cross Section of a specific technology process. Regarding SPICE simulations, these models usually converge into a widely accepted double exponential law for collection current simulation [7] that has been used in the past by several authors for case studies and modeling [8]–[11], but the parameters for the double exponential current are usually selected among typical values referred from the literature or are fixed ad-hoc within certain limits.

In this framework, implementing TCAD and complex physical model approaches to assess Analog Single Event Transients (ASET) sensitivity in an analog circuit, where different transistor sizes, bias conditions and circuit topologies can be found on a single circuit under test (CUT), would increase considerably the time and computational costs in a design stage, when the sensitivity of the circuit is not yet precisely known. In this work, the ASET sensitivity of a full-custom 180nm CMOS operational amplifier is assessed by means of a SPICE based approach but using a tool flow that considers the technological implementation of the circuit and the interaction of a given population of ions with the material stack of the IC. Sensitivity results are obtained through a probabilistic

A. Fontana, S. M. Pazos, F. L. Aguirre and F. Palumbo are with the Microelectronics Laboratory, Electronics Engineering Department, Universidad Tecnológica Nacional, Facultad Regional Buenos Aires, Medrano 951, CABA, Argentina (e-mail: afontana@frba.utn.edu.ar,spazos@frba.utn.edu.ar, faguirre@frba.utn.edu.ar)

S. M. Pazos, F. L. Aguirre and F. Palumbo are also with the are with Consejo Nacional de Investigaciones Científicas y Técnicas (CONICET), Godoy Cruz 2290 (C1425FQB), Buenos Aires, Argentina, GAIANN, Comisión Nacional de Energía Atómica, Gral. Paz 1499 (1650), San Martín, Provincia de Buenos Aires, Argentina

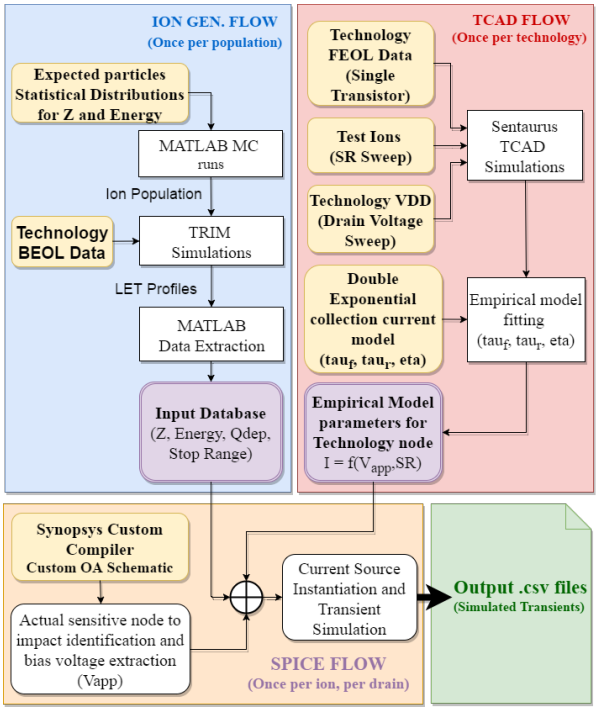


Figure 1: Tool flow used for the sensitivity analysis.

approach and a frequency domain analysis of the induced error pulses at the output of the circuit under test [12]–[14]. The following sections will briefly describe the tool flow and the sensitivity evaluation criteria, followed by the results of the study on the circuit under test.

II. TOOL FLOW

Despite some authors implement a square pulse current source to simulate the current collection due to an ion strike, this approach may have some inaccuracies depending on the frequency response of the stage where the analysis is performed [12]. Therefore, the shape of the current pulse is an important issue to be taken into account in analog circuits. The double exponential model for the collection current [15] is a widely accepted approach for simulating the effects of ASET at the SPICE level. The model basically proposes that the general aspect of the current waveform resulting from the charge collection of an incident particle can be reduced to equation (1), where Q_{coll} is the total collected charge, or the area contained under the current pulse, and τ_f and τ_r are the characteristic rise and fall times of the two exponential components.

$$I(t) = \frac{Q_{coll}}{\tau_f - \tau_r}(e^{\frac{-t}{\tau_f}} - e^{\frac{-t}{\tau_r}}) \quad with \quad Q_{coll} = \eta Q_{dep} \qquad (1)$$

The total collected charge by a sensitive node Q_{coll} can be modeled as a fraction of the total deposited charge (Q_{dep}) through the collection efficiency parameter η or CCE, where the total deposited charge depends on the linear energy transfer (LET) of the incident particle in the substrate, given by (2). η has a strong dependence on the applied voltage, when considering charge collection on a p-n junction, as well as on the charge deposition profile of the particle along the track [16]. This dependence is mainly linked to the width of the depletion region and to its electric field, among other variables.

$$Q_{dep} = \frac{\rho_{Si}}{\frac{w_{ehp_{Si}}}{q}} \int_0^{SR} LET(x)dx \qquad (2)$$

In (3), $LET(x)$ represents the linear energy transfer along the ion track, SR is the stopping range of the incident ion into the substrate, $w_{ehp_{Si}}$ is the energy required to ionize an electron-hole pair in Silicon, i.e. $3.6eV$ per pair, q is the electron charge and ρ_{Si} is the density of Silicon.

Fig. 1 shows a general flow graph of the sensitivity analysis. Three main branches can be identified in this chart. The right branch represents the TCAD simulations of the work flow. Based on the fabrication technology of the CUT, Front-End-Of-Line (FEOL) data is used to create a single transistor structure in Sentaurus TCAD environment. Afterwards, this structure is used to simulate the current transients induced by a test ion by sweeping the Stopping Range (SR) of the ion and the applied drain voltage of the transistor, according to the maximum allowable voltage for the technology. These data is used to fit an empirical model that links the ion's stopping range and the applied voltage on a transistor drain with the parameters of the double exponential current model, i.e. τ_f, τ_r, and Q_{coll} (results not shown). The latter is obtained by fitting the collection efficency parameter η calculated from the TCAD current pulse as Q_{coll}/Q_{dep}. As for the time constants, these where obtained by solving the equation system of IMAX-TMAX according to [15], so that the model pulses hold true the conditions for identical total collected charge, current peak and peak time.

The left branch of the flow graph represents the ion generation for the sensitivity assessment of the CUT. A MATLAB script generates a Monte Carlo population of ions with user-specified energy and species, according to a previously defined statistic distribution, and launches the simulation of the interaction of each generated ion with the CUT material stack using the program TRIM. In this case, the target is a typical BEOL stack of the technology under study, i.e. 180nm bulk CMOS, with its silicon substrate. TRIM launches a series of simulations and generates energy deposition results along the stack, among other results that are not used at the moment by our tool. The MATLAB application extracts the results for the energy deposition in the area of interest, i.e. the substrate. Fig. 2 shows a typical energy loss profile along the stack for an alpha particle at 7.5MeV. With this profile, SR and Q_{dep} are calculated and exported into a CSV database with the ion information, and this database is forwarded to the SPICE tool.

The SPICE tool, implemented in Synopsys Custom Compiler®, receives both the double exponential parameter models obtained in TCAD and the TRIM ion simulation results. With this information, the tool proceeds to identify every sensitive node in the hierarchy of a complex circuit, i.e. transistor drains. Afterwards, node DC bias point is extracted to determine the applied voltage (V_{app}) at the drain junction, alongside with the transistor type (P or N channel). Then, for every generated ion in the database, the tool creates a

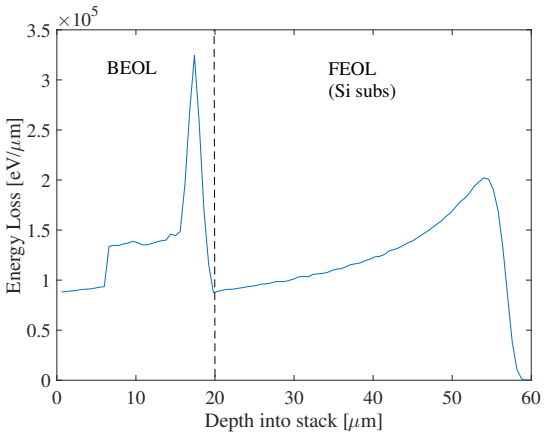


Figure 2: Energy deposition of a 7.5MeV alpha particle along the BEOL/FEOL stack of a 180nm CMOS bulk technology.

double exponential current source (implemented as two current sources in parallel with opposing polarities) and connects it to the node under test. The current shape is determined through the empirical model parameters using the ion SR and the node V_{app}. The output of the circuit is monitored in a transient analysis and characteristic data of the pulses is saved into an output database along with the input ion data. This process is repeated for every sensitive node and every generated ion of the input database. Collected information allows to correlate the signal response of the CUT to the physical input of the system, i.e. the ion information and the impacted transistor, for a given DC bias condition.

III. Fault detection criterion

Currently, there is no general agreement in the scientific community on how to determine the occurrence of a fault in an analog integrated circuit if an ASET takes place, mainly because of the many variables involved on such analysis (impact location, fabrication characteristics, circuit gain, biasing and bandwidth, etc.). A commonly used approach would be to establish an arbitrary threshold voltage for the amplitude of the transient response at the output node. Therefore, a fault will exist if the output voltage at that node exceeds the previously defined threshold voltage. Despite such criterion is useful when trying to asset the influence of a single device on the output variation, it is not enough to address the possible faults the ASET may induce on the system. Since ASET circuit response is closely related to the surrounding system, this becomes an important issue when analyzing the reliability of mixed-signal circuits. The propagation of the ASET to the digital circuitry (becoming a SEU) is jointly determined by pulse's width and duration [17]. Aiming to develop a criterion that takes this effect into account it has been proposed to create a classification evaluating both, the pulse amplitude and width at half minimum, allowing to identify vulnerabilities in the circuit for future hardening [12]. However, this classification has two main inconvenients: on one hand, it provides reduced useful information on large amounts of data, and on the other hand, pulse width for complex signals are quite difficult to consistently determine.

Another very attractive method results by implementing the signal processing theory to the radiation analysis [13]. This approach allows to understand the general variations of ASET waveforms and how pulse propagation mechanisms work, by linking the pulse spectrum with the circuit frequency transfer [12] (i.e. the bandwidth of the target device will attenuate the high frequency components of the pulse spectrum for the downstream system). Besides, based on the pulse energy, this method provides a figure of merit useful to carry out comparisons of vulnerabilities between similar circuits.

The ASET analysis is performed using a simulation data set that hits every transistor of the circuit. The voltage transient of the output of the CUT is measured for the i_{th} different impacting ion on the drain of the j_{th} MOS transistor, converted to the frequency domain by calculating the Fast Fourier Transform ($X_{j,i}(f)$), and bandlimited to the lowest bandwidth of the system [14]. The resulting signals has the potential to propagate to other circuits. The energy spectral density may be used, for each impact, to reveal the frequency components of an ASET that contributes the most error energy, by squaring the magnitudes of the discrete frequency samples. With the purpose of providing an overview of the vulnerability of the circuit, it is possible to obtain an average energy spectral density by using (3) and calculate the total energy contained using (4). This energy brings a measure of the average energy contribution by single events transients in a device, and can be used as a figure of merit. This metric is useful to quantify the radiation sensitivity of the CUT, and to compare it against other possible implementations.

$$ESD_p = |X_p(f)|^2 = \frac{\sum_{j=1}^{m}\sum_{i=1}^{n}|X_{j,i}(f)|^2}{m.n} \tag{3}$$

$$E_{p_{ASET}} = \int_{-\infty}^{\infty}|X_p(f)|^2 df \tag{4}$$

During the design stage, it might be useful to consider the marginal contribution of each transistor, i.e. the energy of the output pulse for the i_{th} different impacting ion for each different MOSFET's drains against the total energy (5). Consequently the transistors prone to cause a significant ASET can be taken into account to reduce its influence on the total response. Similarly, the most hazardous ions can be identified considering the marginal contribution of each ion.

$$E_j\% = \frac{\int_{-\infty}^{\infty}\sum_{i=1}^{n}|X_{j,i}(f)|^2 df}{\int_{-\infty}^{\infty}\sum_{j=1}^{m}\sum_{i=1}^{n}|X_{j,i}(f)|^2 df}.100 \tag{5}$$

At system level, the ion strikes produce voltage fluctuations on the device that can be understood as random noise. Usually, all the systems are designed to tolerate some amount of input and internal noise. Therefore, this specification can be used as a signal bound that allows to determine when an error is produced by comparing it to the frequency spectrum of the pulse. The portion of the SET spectral content that is outside of the system signal bound spectrum is called the SET error energy, and is used as an indicator of the impact of an ASET to the system. This criterion uses for computation, an error measure known as the integral square error (ISE), and the operation is made for every impact simulated on the circuit.

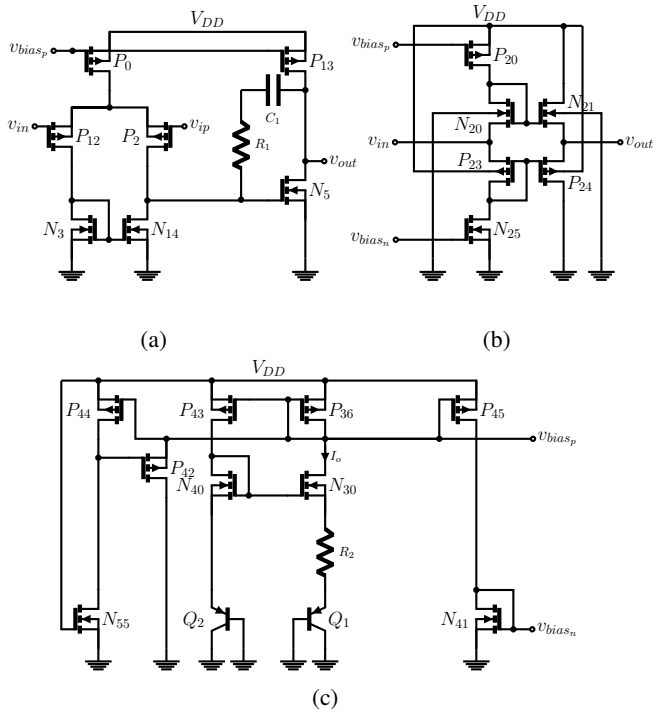


Figure 3: Circuit schematic of the evaluated OpAmp: (a) shows the compensated two stage Miller OTA, (b) the output buffer and (c) the current reference.

If the error energy for a given pulse is higher than zero, then an error occurs. Therefore, probability density functions (PDF) can be obtained, by normalizing histograms of error counts versus error energies or LET. This information enables a system designer to compare multiple similar circuits using the probability of the occurrence of a single event induced error. In addition, this method allows to estimate the error rate of the system for use in a given radiation environment, by calculating the error cross-sections and determining the flux of particles. The error cross-section of a circuit is the total sensitive area that generates an error for particles at each LET of interest. The flux of particles can be obtained from CRÈME 2009 [18], a very powerful tool that models the radiation environment at near Earth orbits.

IV. OpAmp ASET sensitivity assessment

The proposed tool flow and sensitivity characterization procedure described in the previous sections was implemented to asses the ASET sensitivity of a fully custom designed, buffered Miller operational amplifier. The schematic of the circuit under test is shown in Figure 3. Because the selected analysis environment for this device was the geosynchronous orbit, a database of 357 ions was created by taking into account the interaction between the particles in this environment and the technology of the device. The energies and species present in geosynchronous orbit, were randomly assigned between 0 and 500MeV for energy, and Z from 1 to 26 (H to Fe) considering the "iron threshold" [19]. This database was used to generate current pulses at each drain of every transistor in the circuit, implementing a double exponential law that

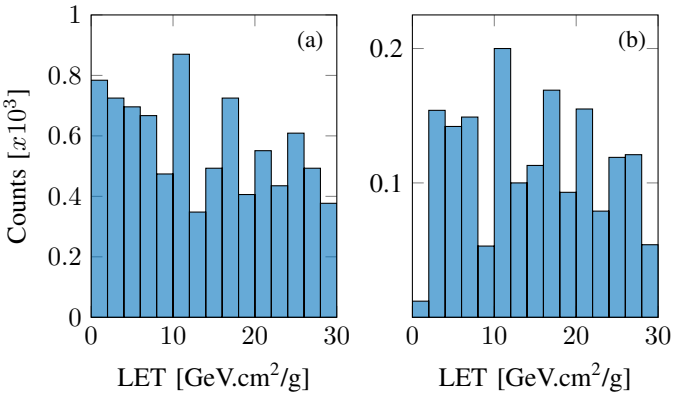


Figure 4: Total observations of events as a function of the ion expected LET (a) and the subset of events that are actually considered as errors with the signal bound criteria (b).

contemplates the collection efficiency. Figure 4 shows an histogram of the expected LET of each particle in 4a and the subset of ions that generated an error in the circuit, according to the signal bound criteria, in 4b. It is possible to observe that although a great amount of ions show low LET values, very few of them finally generate an error in the circuit, and error counts are randomly distributed around the higher LET values.

A wide spread of stopping ranges was found for the particle sample under study for a wide distribution of energies and LET (results not shown). Nevertheless, not only the higher energy particles are responsible for errors. Those particles with stopping ranges very close to the drain junction depth, yielding high efficiency values, can be responsible for a large amount of errors. Therefore, it is not mandatory for a particle to have a high energy or high LET value to create an error, as if a large portion of the particle energy is deposited close to the surface, charge collection will be highly efficient and have good probabilities to induce an error.

Among the results, device sensitivity in the circuit is of

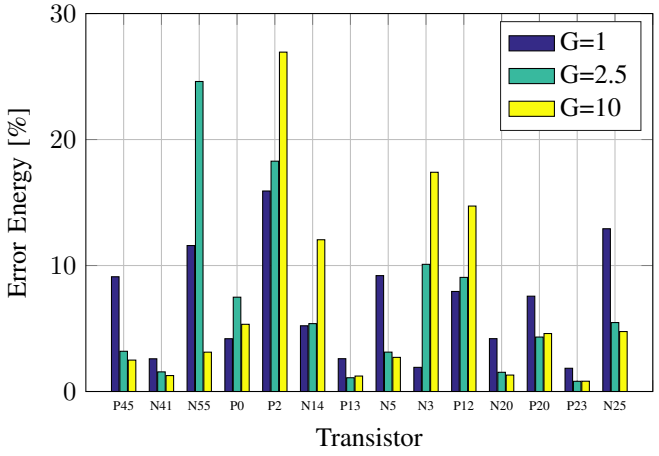


Figure 5: Relative Error energy of each tansistor in the circuit for three different closed loop gains. Only those transistor with error energies above 1% are shown.

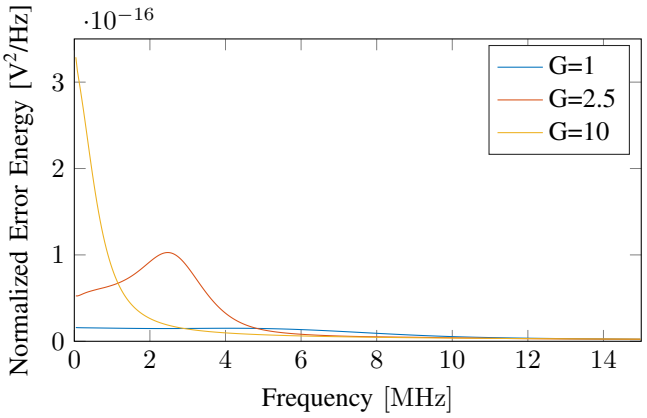


Figure 6: Normalized Error Energy vs. frequency of the averaged error pulses for non-inverting gain configurations of 1, 2.5 and 10.

utmost importance to introduce hardening strategies for the circuit. Figure 5 shows the error energy proportion linked to each transistor of the circuit. For the sake of clarity, only those transistors showing error energies above 1% are displayed in the histogram. Results are shown for 3 different non-inverting gain configurations. This plot shows that most sensitive transistor in the circuit for each gain is the differential input transistor P2. It is interesting to observe that the gain configuration tends to desensitize certain devices in the circuit and increase the sensitivity of others. Transistors N25 and N3 are good examples of this behavior. Table I depicts the overall average energy of each closed loop configuration, used as a figure of merit of the radiation sensitivity of the circuit.

The average ESD for the three gain configurations are shown in Figure 6. It can be seen that for higher gains the error energy tend to focus in the lower frequencies. This is a logical result as the bandwidth of the amplifier is reduced for higher gains, ergo limiting the harmonic content of the resulting output error pulses.

At system level, Figure 7 highlights the resulting error output transient pulses for the three most hazardous ions identified on the most sensitive transistor of the circuit P2 in buffer configuration (unit gain). The energy distribution of the pulses in the frequency domain are compared against the signal bound of the system in Figure 8. The noise tolerance specifications for the selected system was a composite of the maximum input noise signal tolerated (a rectangular pulse of 200mV and 50ns) and an internal RMS noise floor of $3\frac{nV}{\sqrt{Hz}}$. Considering the total amount of observed errors and the integral of the energy that results in each one of them, the probability of each

Table I: Figures of merit for different gain configurations.

CONFIGURATION	FIGURE OF MERIT [pV^2]
Non-inverting G=1	194.63
Non-inverting G=2.5	385.92
Non-inverting G=10	343.35

measured level of error energy that produces an actual error can be plotted as shown in figure 9. Higher probabilities can be found for lower error energies, suggesting that most of the observed errors are produced by low total energy pulses. This result evidences that a small reduction of circuit sensitivity (i.e. a larger signal bound), when possible, can strongly lower the error probability, requiring very high energy pulses to produce an actual detectable error.

V. Conclusion

In this work, a SPICE based ASET sensitivity assessment of a full custom 180nm CMOS OpAmp is presented. The proposed evaluation flow proposes the automation of the several tools that involve the solution of the particle-matter interaction for a given technology, the generation of double exponential current pulses according to the ion energy deposition profile and the biasing conditions of the sensitive device, the automatic injection of SET into every sensitive node of the circuit and the summary of figures of merit for the circuit under test by considering a frequency domain, error energy approach for a given system specification, like the one proposed in [13].

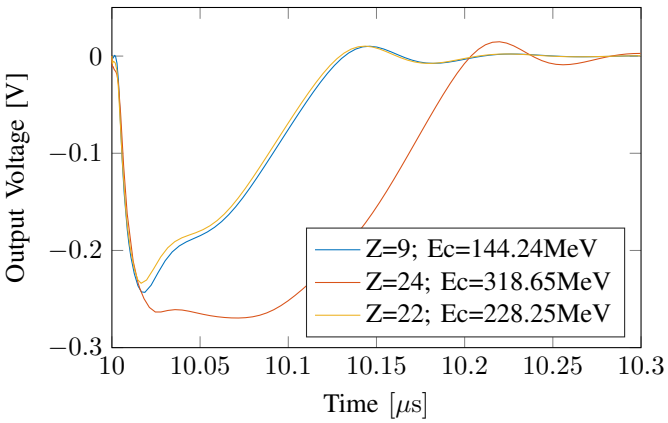


Figure 7: Output error transient examples for three different ions impacting on the same transistor.

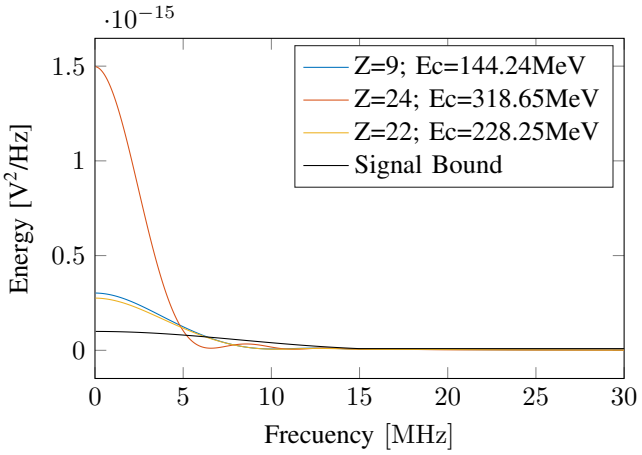


Figure 8: Output error pulses energy distribution in the frequency domain compared wih the frequency representation of the signal bound. Area above this bound is considered error energy.

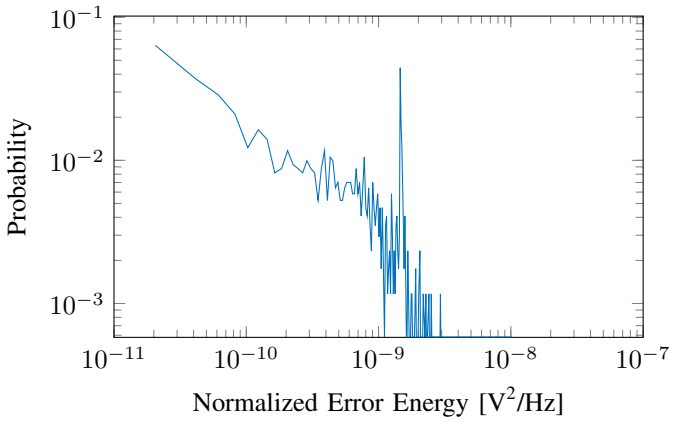


Figure 9: Probability of error as a function of normalized error energy. Lower energy pulses are responsible for most of the errors.

Overall results are consistent with previously reported data on simulations of bipolar technology operational amplifiers [12]–[14]. Nevertheless, these works consider a parametric approach to consider different LET values and consider much different overall values ascribed to higher signal bounds of the circuit under study. Our approach adds information to the sensitivity analysis by selecting a given radiation environment, considering an actual population of ions and its effects on a given technology, in an attempt to obtain a more accurate analysis of the circuit and the system involved.

Simulation results allow not only to identify the most sensitive devices but also gives a general characterization of the circuit sensitivity and particles involved in the most observed errors. The definition of a tolerance bound for the system can be critical for the final error probability of a circuit placed in a given radioactively aggressive environment. For the circuit under test, sensitive transistors were identified to be P2, P12, N3 and N55 but the amplifier feedback configuration must be taken into account as some transistors may become more sensitive according to the closed-loop configuration.

It is important to consider that not only high energy or high LET value particles will always induce an error. The influence of the charge deposition profile should be taken into account, mainly for analog circuits. Simulation results can be further normalized to environment conditions by considering a given particle flux, and make estimations of error rate of the system for the given environment.

In order to validate the simulation tool, several experimental tests will be performed on the Microbeam of the TANDAR Laboratory in CNEA. This heavy-ion accelerator has a wide range of ion species and energies available, and allows the characterization of SET by the irradiation of every transistor of the device shown in this work. Finally, simulations of the particles and energies used will be checked against the experimental results.

Acknowledgment

The authors would like to thank Dr. Mariano Llamedo Soria, Dr. Mario Debray and Lic. Nahuel Vega for the inspiring discussions.

References

[1] L. Artola, M. Gaillardin, G. Hubert, M. Raine, and P. Paillet, "Modeling single event transients in advanced devices and ics," *IEEE Transactions on Nuclear Science*, vol. 62, no. 4, pp. 1528–1539, Aug. 2015.

[2] J. Wallmark and S. Marcus, "Minimum Size and Maximum Packing Density of Nonredundant Semiconductor Devices," in *Proceedings of the IRE*, vol. 50, no. 3. IEEE, Mar. 1962, pp. 286–298.

[3] E. L. Petersen, R. Koga, M. A. Shoga, J. C. Pickel, and W. E. Price, "The Single Event Revolution," *IEEE Transactions on Nuclear Science*, vol. 60, no. 3, pp. 1824–1835, Mar. 2013.

[4] Y. Zhao, L. Wang, S. Yue, D. Wang, X. Zhao *et al.*, "SEU and SET of 65nm Bulk CMOS Flip-flops and Their Implications for RHBD," *IEEE Transactions on Nuclear Science*, vol. 62, no. 6, pp. 2666–2672, Dec. 2015.

[5] J. R. Ahlbin, M. J. Gadlage, D. R. Ball, A. W. Witulski, B. L. Bhuva *et al.*, "The Effect of Layout Topology on Single-Event Transient Pulse Quenching in a 65 nm Bulk CMOS Process," *IEEE Transactions on Nuclear Science*, vol. 57, no. 6, pp. 3380–3385, Dec. 2010.

[6] R. A. Reed et al., "Anthology of the Development of Radiation Transport Tools as Applied to Single Event Effects," *IEEE Transactions on Nuclear Science*, vol. 60, no. 3, pp. 1876–1911, Jun. 2013.

[7] T. Heijmen, D. Giot, and P. Roche, "Factors That Impact the Critical Charge of Memory Elements," in *12th IEEE International On-Line Testing Symposium (IOLTS'06)*. IEEE, Jul. 2006, pp. 57–62.

[8] F. J. Franco, C. Palomar, J. G. Izquierdo, and J. A. Agapito, "SPICE Simulations of Single Event Transients in Bipolar Analog Integrated Circuits Using Public Information and Free Open Source Tools," *IEEE Transactions on Nuclear Science*, vol. 62, no. 4, pp. 1625–1633, Aug. 2015.

[9] C. Viale, P. Petrashin, L. Toledo, W. Lancioni, and C. Vazquez, "Single event effects in an analog SOI transconductor: a case study," in *2015 16th Latin-American Test Symposium (LATS)*. IEEE, Mar. 2015, pp. 1–4.

[10] D. Fusco and T. R. Balen, "Radiation effects in low power and ultra low power voltage references," in *2016 17th Latin-American Test Symposium (LATS)*. IEEE, Apr. 2016, pp. 111–116.

[11] F. Marquez, F. Munoz, F. R. Palomo, L. Sanz, E. Lopez-Morillo *et al.*, "Automatic Single Event Effects Sensitivity Analysis of a 13-Bit Successive Approximation ADC," *IEEE Transactions on Nuclear Science*, vol. 62, no. 4, pp. 1609–1616, Aug. 2015.

[12] Y. Boulghassoul, L. Massengill, T. Turflinger, and W. Holman, "Frequency domain analysis of analog single-event transients in linear circuits," *IEEE Transactions on Nuclear Science*, vol. 49, no. 6, pp. 3142–3147, Dec. 2002.

[13] A. V. Kauppila, G. L. Vaughn, S. Member, J. S. Kauppila, L. W. Massengill, and B. Qualification, "Probabilistic Evaluation of Analog Single Event Transients," *IEEE Transactions on Nuclear Science*, vol. 54, no. 6, pp. 2131–2136, Dec. 2007.

[14] A. Kauppila, L. Massengill, W. Holman, G. Vaughn, and J. Kauppila, "Frequency-domain analysis of analog single-event transients (ASETs) based on energy spectral density," *IEEE Transactions on Nuclear Science*, vol. 51, no. 6, pp. 3537–3545, Dec. 2004.

[15] F. Wrobel, L. Dilillo, A. D. Touboul, and V. Pouget, "Determining Realistic Parameters for the Double Exponential Law that Models Transient Current Pulses," *IEEE Transactions on Nuclear Science*, vol. 61, no. 4, pp. 1813–1818, Aug. 2014.

[16] M. Friedl, T. Bauer, and M. Krammer, "A simple model of charge collection in silicon detectors," *Nuclear Instruments and Methods in Physics Research Section A: Accelerators, Spectrometers, Detectors and Associated Equipment*, vol. 461, no. 1, pp. 192–196, Apr. 2001.

[17] P. Roche, J. Palau, K. Belhaddad, G. Bruguier, R. Ecoffet, and J. Gasiot, "SEU response of an entire SRAM cell simulated as one contiguous three dimensional device domain," *IEEE Transactions on Nuclear Science*, vol. 45, no. 6, pp. 2534–2543, Dec. 1998.

[18] J. H. Adams, A. F. Barghouty, M. H. Mendenhall, R. A. Reed, B. D. Sierawski *et al.*, "CRÈME: The 2011 Revision of the Cosmic Ray Effects on Micro-Electronics Code," *IEEE Transactions on Nuclear Science*, vol. 59, no. 6, pp. 3141–3147, Dec. 2012.

[19] S. Kayali, G. Ponchak, and R. Shaw, "GaAs MMIC Reliability Assurance Guideline forSpace Applications," Jet Propulsion Laboratory, NASA, Tech. Rep., 1996.